Magnetism

J. Synchrotron Rad. (1999). **6**, 673–675

X-ray natural circular dichroism of gyrotropic crystals

José Goulon,[a]* Chantal Goulon-Ginet,[a,b] Andrei Rogalev,[a] Vincent Gotte,[a] Cécile Malgrange[c] and Christian Brouder[c]

[a]European Synchrotron Radiation Facility, B.P. 220, F-38043 Grenoble Cedex, France, [b]Faculté de Pharmacie, Université Joseph Fourier, Domaine de la Merci, F-38700 La Tronche, France, [c]Laboratoire de Minéralogie Cristallographie, Universités Paris VI et VII, Case 115, 4 Place Jussieu, F-75252 Paris Cedex 05, France. Email:goulon@esrf.fr

We review the conditions under which Natural Circular Dichroism can be observed in the X-ray range for either uniaxial or biaxial gyrotropic single crystals.

Keywords: optical activity, circular dichroism, X-ray absorption spectra

1. Introduction

Over one century after the discovery of X-rays (Röntgen, 1895) and the discovery of circular dichroism (CD) in absorption bands (Cotton, 1895), we have produced the first experimental evidence of *Natural* CD in the X-ray range (Goulon *et al.*, 1998; Alagna *et al.*, 1998). Such experiments became possible with the third generation Synchrotron Radiation sources and, more specifically, with the development of powerful helical undulators which can produce intense fluxes of X-rays with a full control of their polarization state (Elleaume, 1994). Whereas X-ray Magnetic Circular Dichroism (XMCD) spectra are most easily recorded by reversing the direction of the applied magnetic field (Schütz *et al.*, 1987), it is essential in X-ray Natural Circular Dichroism (XNCD) experiments to reverse the sign of the Stokes-Poincaré component P_3 : this is where our helical undulator Helios-II is particularly appropriate. The recent development of X-ray quarter-wave plates made it also possible to measure accurately the polarization rates of the incident X-ray beam (Goulon *et al.*, 1996) whereas the polarization transfer function of Bragg monochromators can now be predicted very accurately. On the other hand, there was rather little motivation to look for natural optical activity in the X-ray range because the Rosenfeld rotatory strength is expected to vanish in inner shell spectroscopies. There are several reasons for that : (i) Magnetic Dipole (M1) transitions are forbidden due to the orthogonality of the core and valence orbitals ($\Delta n = 0$ selection rule); this is even more restrictive for spectra recorded at K (or L_1) edges because no magnetic dipole transition is allowed from a pure 1s (or 2s) atomic state while the energy separation between deep core levels makes 1s,2p hybridization quite improbable; (ii) the sum over all spin orbital projections of the core electrons results in a kind of internal optical sum rule so that the measured dichroism should systematically yield zero. We realized that natural circular dichroism could nevertheless be observed with gyrotropic single crystals due to the substantial contribution in the X-ray range of the Electric Dipole-Electric Quadrupole (E1.E2) interference terms first investigated by Barron at optical wavelengths (Barron, 1971). We will discuss first which crystal class is appropriate to detect XNCD and we will give a general formulation of the XNCD cross sections σ (E1.E2).

2. X-ray gyrotropy in non-centrosymmetrical crystals

Looking for the rotational invariants in O_3^+ of the rank-3 optical activity tensor γ_{ijk} , one is led to a decomposition including a scalar, a vector and a rank-2 pseudodeviator parts.

Table 1
Rotational invariants of γ_{ijk} for the 21 non-centrosymmetrical crystal classes.

Crystal classes	Point groups	Enantiomorphism		XNCD
		Pseudo-scalar	Vector	Pseudo-deviator
$\bar{4}3m$ $\bar{6}m$ $\bar{6}$	T_d D_{3h} C_{3h}	no	no	no
432 23	O T	yes	no	no
622 32 422	D_6 D_3 D_4	yes	no	yes
$6mm$ $3m$ $4mm$	C_{6v} C_{3v} C_{4v}	no	yes	no
6 3 4	C_6 C_3 C_4	yes	yes	yes
$\bar{4}2m$	D_{2d}	no	no	yes
$\bar{4}$	S_4	no	no	yes
$mm2$	C_{2v}	no	yes	yes
222	D_2	yes	no	yes
2	C_2	yes	yes	yes
m	C_s	no	yes	yes
1	C_1	yes	yes	yes

At optical wavelengths, both the scalar and the pseudodeviator parts contribute to detectable optical activity whereas, in the X-ray range, *only the pseudodeviator part* induces natural optical activity. Following Jerphagnon and Chemla (1976), we have summarized in table 1 which ones of the 21 non-centrosymmetrical crystal classes are compatible with XNCD. Note that there are only two crystal classes (432 ; 23) which have a non zero pseudoscalar part but no pseudodeviator term: such crystals are optically active in the visible but will not exhibit any XNCD. Thus, only 13 crystal classes will exhibit XNCD. Hereafter, we will consider two crystals which both exhibit a large non-linear susceptibility at optical wavelengths: α-$LiIO_3$ is uniaxial (class 3) and belongs to an enantiomorphous crystal class whereas $KTiOPO_4$ (KTP) belongs to the biaxial non-enantiomorphous crystal class *mm2*.

The X-ray absorption cross section associated with the E1.E2 interference term can be written :

$$\sigma_{NCD} = (4\pi)^2 \alpha_0 \hbar\omega\, k\, P_3 \sum_f \varepsilon_{\alpha\beta\lambda} \kappa_\lambda \kappa_\gamma \langle g|r_\alpha|f\rangle\langle f|r_\beta r_\gamma|g\rangle \times \delta(E_f - E_g - \hbar\omega)$$

© 1999 International Union of Crystallography
Printed in Great Britain – all rights reserved

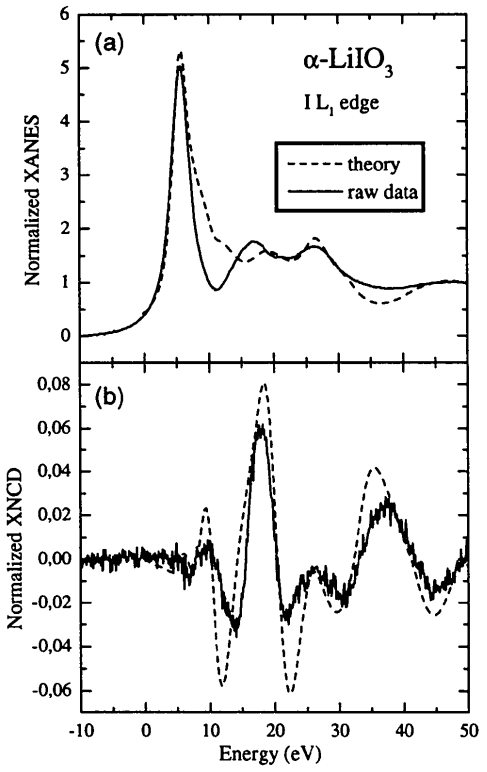

Figure 1
a) Comparison of the experimental and simulated L_1 edge XANES spectra of α-$LiIO_3$.
b) Comparison of the experimental and simulated L_1 edge XNCD spectra of α-$LiIO_3$.

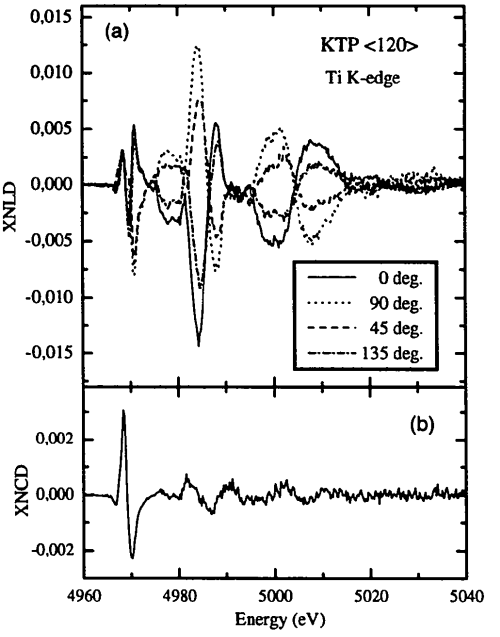

Figure 2
a) Linear dichroism contaminating the measured CD spectra of KTP <1,2,0>.
b) Extracted XNCD signal.

where α_0 is the fine structure constant, $\varepsilon_{\alpha\beta\lambda}$ is the Levi-Civita alternating tensor and the κ_λ are the components of the unit wavevector. For a powder or a solution, the orientational average: $<\sigma_{NCD}>=0$ and there is no XNCD. This is due to the fact that the Wigner rotation matrices respectively associated with E1 and E2 are orthogonal.

3. Results

The *Fluorescence Detected* X-ray absorption near edge spectrum (XANES) of α-$LiIO_3$ measured at the L_1 edge of iodine is reproduced in Fig.1a whereas the corresponding XNCD signal $[\sigma_L - \sigma_R]$ is displayed in Fig.1b. The largest XNCD signal is not found in the white line but for the next resonance peaking from 12 eV toward higher energy. The amplitude of the XNCD signal is rather large: up to 5.5 % after proper correction for the polarization transfer of the monochromator. Note that there is a fairly encouraging agreement between the experimental XANES or XNCD data and the spectra simulated using *ab initio* calculations performed within the framework of the Multiple Scattering theory. On the other hand, the XNCD spectra recorded at the L_2 and L_3 edges have the same sign and are looking very similar (Goulon *et al.*, 1998): this is in contrast with XMCD spectra which, most often, exhibit opposite sign. While the exchange and spin-orbit interactions are the driving terms in XMCD, this is not the case in XNCD and our data leave very little or no hope to detect any contribution of the scalar E1.M1 interference term.

As illustrated by Fig.2a, the case of biaxial crystals is far more complicate because the tiny effects of X-ray gyrotropy are swamped by large linear dichroism signals (XNLD) mostly due to the imperfect polarization transfer of Bragg monochromators (Goulon *et al.*, 1999). Since the contribution of gyrotropy is invariant in a rotation around the wavevector of the incident beam, the true XNCD signal can be extracted from the angular dependence of the spectra (Fig.2b). There is another complication: light propagating inside a biaxial crystal does not keep a constant polarization state. This can be taken into account using the differential equation (Goulon *et al.*, 1999):

$$\frac{\partial}{\partial z}|\mathbf{S}\rangle = a\mathbf{M}|\mathbf{S}\rangle \quad \text{with} \quad \mathbf{M} = \begin{bmatrix} t' & u' & -v' & w \\ u' & t' & -w' & v \\ -v' & w' & t' & u \\ w & -v & -u & t' \end{bmatrix}$$

where $|\mathbf{S}\rangle$ is the Stokes vector for a penetration depth z whereas $\mathbf{M}$ is a 4x4 differential Müller matrix in which the coefficients u, u', v , v', w and w' can be related to the anisotropic components of the multipolar polarizability tensors at the absorbing site (Goulon *et al.*, 1999). It should be underlined that $\{w,w'\}$ are the only terms that contain any information on the time-even,

antisymmetric part of the microscopic gyrotropy tensor, whereas $\{u,u'\}$ and $\{v,v'\}$ describe the anisotropy of the electric dipole (E1.E1) and electric quadrupole (E2.E2) terms in non-magnetic crystals. One is led to the following expression of the *Fluorescence-Detected* XNCD spectra :

$$\mathbb{S}_0^3 = -2P_3^0 S_0^0 \Gamma_{00}^F(\varphi)\{w\mu + [wt'+(u'v - v'u)]\mu^2 + \varepsilon(\mu^3)\}$$

where: $S_3^0 = P_3^0 S_0^0$ is the circular Stokes component of the incident X-ray beam, $\Gamma_{00}^F(\varphi)$ is the quantum yield of X-ray fluorescence emitted in a direction characterized by the wavevector $\mathbf{k}_F$ that can be deduced from the wavevector $\mathbf{k}$ of the incident beam by a rotation φ in the scattering plane. On the other hand, μ refers to the usual correction for reabsorption with : $1/\mu = -(t'+t'_F)$ where at' and at'_F stand for the isotropic absorption cross sections at the energies of the incident photons and fluorescence photons respectively. We wish to emphasize that there are certainly biaxial crystals for which $uv'-vu' \neq 0$ *i.e.* the anisotropy of the dipolar electric polarizability may contribute to a second order circular dichroism that is not related to gyrotropy. We found, however, that this additional dichroism, first predicted by Born and Huang (1954), should be small in *Fluorescence-Detected* XNCD experiments.

References

Alagna, L., Prosperi, T., Turchini, S., Goulon, J., Rogalev, A., Goulon-Ginet, C., Natoli, C.R., Stewart, B. & Peacock, R.D. (1998). *Phys. Rev. Lett.* **80**, 4799-4802.

Barron, L.D. (1971). *Molecular Physics* **21**, 241-246.

Born, M. & Huang, K. (1954). In *Dynamical Theory of Crystal Lattices*, Clarendon-Oxford, pp. 336-38.

Cotton, A. (1895). *C. R. Acad. Sci. (Paris)* **120**, 989-1044.

Elleaume, P. (1994). *J. Synchrotron Rad.* **1**, 19-26.

Goulon, J., Malgrange, C., Gilès, C., Neumann, C., Rogalev, A., Moguiline, E., De Bergevin F. & Vettier, C. (1996). *J. Synchrotron Rad.* **3**, 272-281.

Goulon, J., Goulon-Ginet, C., Rogalev, A., Gotte, V., Malgrange,C., Brouder, Ch. & Natoli, C.R. (1998). *J. Chem. Phys.* **108**, 6394-6403.

Goulon, J., Goulon-Ginet, C., Rogalev, A., Gotte, V., Brouder, Ch. & Malgrange, C. (1999). *Submitted to J. Opt. Soc. Am. B.*

Jerphagnon, J. & Chemla, D.S. (1976). *J. Chem. Phys.* **65**, 1522-1529.

Röntgen, W.C. (1895). Communication to the Würtzburg Physical & Medical Society.

Schütz, G., Wagner, W., Wilhelm, W., Kienle, P., Zeller, R., Frahm, R. & Materlik, G. (1987). *Phys. Rev. Lett.* **58**, 737-740.

(*Received 10 August 1998; accepted 3 December 1998*)